

Modeling the power of an optical parametric generator by discrete mode summation

S. Acco · A. Arie · Y. Ben-Aryeh · M. Katz · P. Blau

Received: 10 January 2010 / Revised version: 15 January 2011 / Published online: 16 March 2011
© Springer-Verlag 2011

Abstract An analytical expression for calculating the signal output power of an optical parametric generator (OPG) configuration was developed. The model is based on Heisenberg equations in space and radiation mode theory. A simple analytical expression can be obtained by assuming that all modes within the gain bandwidth of the nonlinear crystal have the same gain and the same interaction length. Another derivation considers the gain and interaction length of each individual mode. The model predictions are in excellent agreement with the measured signal power of OPGs based on 25- and 35-mm periodically poled LiNbO₃ crystal (with effective quadratic nonlinearity of ~ 14.5 pm/V) and 47-mm periodically poled LiTaO₃ crystal (with effective quadratic nonlinearity of ~ 9 pm/V). In addition, a comparison was made between the summation over discrete modes approach and the traditional approach of continuous integration over the beam parameters and pump frequency. We have found that the first approach, which is developed in this paper, predicts more accurately the output power of the OPG.

1 Introduction

An optical parametric generator (OPG) is a high gain, single pass parametric amplifier that generates signal and idler

fields by nonlinear interaction between the pump field and the quantum noise. Parametric fluorescence was first analyzed in 1961 by Louisell et al. [1]. Their derivation provided the expectation value for the photon numbers of the signal and idler. However, this calculation was limited to only a single mode of the signal and idler, but, since OPGs may have $\sim 10^4$ different modes, further analysis was needed to derive the total generated OPG power.

In 1967 Giallorenzi and Tang [2] described the parametric fluorescence as a scattering problem in nonlinear crystals. Following the general procedure in quantum field theory, an expression for the scattering coefficient was obtained. The coefficient defined the ratio between the number of photons spontaneously emitted into a differential solid angle and frequency interval, due to parametric scattering (per unit time, per unit volume) and the incident pump photon flux. The total power is obtained by summing over the angles and frequencies.

In 1968 Byer and Harris [3] treated the onset of the parametric process as parametric amplification of signal and idler waves from noise photons. They assumed that in each mode one photon was created by optical parametric fluorescence at the entrance plane of the crystal and was amplified by the pump.

Although many publications analyzed the operation of an OPG [4–7], most of them showed good agreement with experimental measurements only for the very low gain–length product regime $gL \approx 10^{-3}$, where g is the parametric gain and L is the crystal length. In most of the works, the small signal gain approximation was taken into account.

In this work we propose two different approaches for summing the contributions of different modes to the total OPG power. By considering the finite interaction volume, set by the pump cross-sectional area and crystal length, one can quantize the modes of the signal and idler. The first ex-

S. Acco (✉) · M. Katz · P. Blau
Electro-Optics Division, Soreq NRC, Yavne 81800, Israel
e-mail: optics3@gmail.com

S. Acco · A. Arie
Department of Physical Electronics, School of Electrical Engineering, Tel-Aviv University, Tel-Aviv 69978, Israel

Y. Ben-Aryeh
Physics Department, Technion—Israel Institute of Technology, Haifa 32000, Israel

pression that calculates the OPG signal power has analytical form and is obtained by assuming equal gain and identical interaction length for all modes that propagate in the gain bandwidth of the nonlinear crystal.

The second approach for calculating the signal output power was developed by considering the finite interaction volume, set by the pump cross-sectional area and crystal length; one can quantize the modes of the signal and idler. For each pair of signal and idler modes, one can calculate the phase mismatch, the parametric gain and the corresponding number of photons. By summing over all these discrete modes, the OPG output power is obtained. This method of discrete summation over the electromagnetic modes is more accurate than previous methods [7, 8] that relied on integration over the physical parameters of the beam (namely, its angular and radial coordinates and its frequency), since each mode is characterized by a different parametric gain.

In Sect. 2 detailed derivations of the theoretical models are presented; we start by deriving the photon number of a single mode at the output facet of the crystal, and then evaluate the number of modes in a volume defined by the crystal length and pump beam diameter. In the first model, identical gain for all modes that propagate in the gain bandwidth of the nonlinear crystal was assumed for calculating the signal output power of the OPG.

The second model is based on discrete summation of all the electromagnetic modes that are parametrically amplified in the OPG. This enables us to estimate the phase mismatch, the effective interaction length and consequently the parametric gain for each mode. Summing the contributions of all modes provides the signal output power of the amplifier. In Sect. 3 the experimental setup for the OPG configuration and the measurement technique are described. In Sect. 4 we compare the theoretical and experimental results and conclude with a short summary in Sect. 5.

2 Theoretical model: mode by mode contribution to OPG power

2.1 Calculating the photon number of a single mode of the OPG

It is well known from quantum field theory that the generator for time evolution is the Hamiltonian \hat{H} that satisfies the equation of motion in the time picture [9]:

$$i\hbar \frac{\partial \hat{O}(z, t)}{\partial t} = [\hat{O}(z, t), \hat{H}], \quad (1)$$

where the Hamiltonian \hat{H} is obtained by integrating the Hamiltonian density H over the volume V . The Hamiltonian which describes the energy of the system does not have directionality. The spatial dependence of each electromagnetic

mode does not enter in the time-dependent equation of motion (1). The common approach for describing propagation in quantum mechanical systems is to use a Hamiltonian for the volume V and relate time and space by the velocity of propagation (e.g. $z = vt$). This approach is valid only for cases in which all the waves are propagating with the same velocity. Since in our case the propagating waves (pump, signal and idler) do not have the same velocity, this assumption cannot be used.

In the nonlinear crystal the traveling waves each have to be analyzed into an infinity of modes that have different wavelengths and different directions; the time-dependent equation of motion cannot be used. For this purpose, a theoretical method for treating propagation in quantum optics is adopted, in which the momentum operator is used in addition to the Hamiltonian. The equation of propagation is given by [9]

$$-i\hbar \frac{\partial \hat{O}(z, t)}{\partial z} = [\hat{O}(z, t), \hat{G}], \quad (2)$$

where \hat{G} is the momentum operator and $\hat{O}(z, t)$ is the one-dimensional space evolution for the creation and annihilation operators $\hat{a}_\omega(z)$, $\hat{a}_\omega^\dagger(z)$, respectively. The use of the creation and annihilation operators (in (1)) is for a certain wave-vector k where the spatial dependence is unchanging.

The use of (1) is for a constant value of ω and an explicit direction in space, so that the modes with definite k used in (2) (e.g. e^{-ikz} , where $k = \omega(n)/c$ is the wave-vector) are exchanged into modes with definite ω (e.g. $e^{-i\omega t}$) propagating in a definite direction. The formalism we used in this work is more suitable for modes with different frequencies that propagate in different directions.

The two-mode momentum operator for our system is given by [9, 10]

$$\hat{G} = \hbar g (\hat{a}_s^\dagger \hat{a}_i^\dagger \exp(-i\Delta kz) + \hat{a}_s \hat{a}_i \exp(-i\Delta kz)), \quad (3)$$

where $\vec{\Delta k} = \Delta k \cdot \hat{z} = \vec{k}_p - \vec{k}_s - \vec{k}_i - \vec{k}_{\text{QPM}}$ is a vector which is assumed to be in the propagation direction z , k_p , k_s and k_i are the pump, signal and idler wave-vectors and $k_{\text{QPM}} = (2\pi/\Lambda)\hat{z}$ is the quasi-phase-matched reciprocal vector, Λ is the modulation period of the nonlinear coefficient.

The gain coefficient g is given by [11]

$$g = \frac{\omega_s \omega_i |d_{\text{eff}}|^2 |A_p|^2}{n_s n_i c^2} = \frac{2\omega_s \omega_i |d_{\text{eff}}|^2 I_p}{n_s n_i n_p \epsilon_0 c^3}. \quad (4)$$

In these equations, A_p is the pump field, I_p is the peak pump irradiance, h is Planck's constant, ϵ_0 is the dielectric constant in free space, ω and n are the angular frequency and refractive index of the waves, where the subscripts i , s and p refer to idler, signal and pump, d_{eff} is the nonlinear coefficient and c is the speed of light. In (3), the annihilation

and creation operators $\hat{a}^\dagger(t)$ and $\hat{a}(t)$ are exchanged to $\hat{a}^\dagger(z)$ and $\hat{a}(z)$, where z is the one-dimensional propagating distance.

The operators should satisfy the following commutation relations (CR) [12]:

$$\begin{aligned} [\hat{a}_l(z), \hat{a}_m^\dagger(z)] &= [\hat{a}_l(0), \hat{a}_m^\dagger(0)] = \delta_{lm}, \\ [\hat{a}_l(z), \hat{a}_m(z)] &= [\hat{a}_l(0), \hat{a}_m(0)] = 0, \\ [\hat{a}_l^\dagger(z), \hat{a}_m^\dagger(z)] &= [\hat{a}_l^\dagger(0), \hat{a}_m^\dagger(0)] = 0. \end{aligned} \tag{5}$$

Here δ_{lm} is the Kronecker delta symbol and the subscripts m and l denotes the m th and the l th modes.

The expectation values $\langle \hat{a}_s^\dagger(z)\hat{a}_s(z) \rangle$ and $\langle \hat{a}_i^\dagger(z)\hat{a}_i(z) \rangle$ represent the flux of the photon numbers, for the signal and idler, respectively. It is important to notice that any two operators belonging to different modes commute and also annihilation operators (creation operators) commute with annihilation operators (creation operators).

We need to calculate only the numbers of photons in the signal and idler modes at a distance $z = L$ of the crystal, where the initial state at $z = 0$ is the vacuum state $|0\rangle$. It should take into account that while the classical amplitudes for our case vanish at $z = 0$, $\hat{a}_s(z)$ and $\hat{a}_i^\dagger(z)$ represent quantum input operators where the calculation of any expectation value (corresponding to classical measurement) might depend on the order of operators. Any initial operator $\hat{a}_s(0)$ or $\hat{a}_i(0)$ operating directly to the right on the ket vacuum state $|0\rangle$ vanishes. Any initial operator $\hat{a}_s^\dagger(0)$ or $\hat{a}_i^\dagger(0)$ operating directly to the left on the bra state $\langle 0|$ vanishes.

Using (2) and (3) together with the commutation relations (given in (5)), we get the explicit equations of motion for propagation:

$$\begin{aligned} \frac{d\hat{a}_s}{dz} &= ig\hat{a}_i^\dagger \exp(-i\Delta kz), \\ \frac{d\hat{a}_i^\dagger}{dz} &= -ig\hat{a}_s \exp(i\Delta kz). \end{aligned} \tag{6}$$

Equations (6)–(5) are linear equations, so they can be solved in term of initial conditions for $\hat{a}_s(0)$ and $\hat{a}_i(0)$ at $z = 0$. It should be noted that our model neglects the losses of the signal and idler waves; otherwise, it would become very difficult to solve them analytically.

In order to determine the OPG output power, we need to calculate only the numbers of photons in the signal and idler modes at a distance $z = L$ of the crystal, where the initial state at $z = 0$ is the vacuum state $|0\rangle$. It should be noted that while the classical amplitudes for our case vanish at $z = 0$, $\hat{a}_s(0)$ and $\hat{a}_i^\dagger(0)$ represent quantum input operators, and the calculation of any expectation value (corresponding to classical measurement) might depend on the order of operators. Any initial operator $\hat{a}_s(0)$ or $\hat{a}_i(0)$ operating directly to the

right on the ket vacuum state $|0\rangle$ vanishes. Any initial operator $\hat{a}_s^\dagger(0)$ or $\hat{a}_i^\dagger(0)$ operating directly to the left on the bra state $\langle 0|$ vanishes. The solution of the two operator equations (3) is given by

$$\begin{aligned} \hat{a}_s(z) &= \left\{ \hat{a}_s(0) \left[\cosh(bz) + i\frac{\Delta k}{2b} \sinh(bz) \right] \right. \\ &\quad \left. + i\frac{g}{b}\hat{a}_i^\dagger(0) \sinh(bz) \right\} \exp\left(-i\frac{1}{2}\Delta kz\right), \\ \hat{a}_i^\dagger(z) &= \left\{ \hat{a}_i^\dagger(0) \left[\cosh(bz) - i\frac{\Delta k}{2b} \sinh(bz) \right] \right. \\ &\quad \left. - i\frac{g}{b}\hat{a}_s(0) \sinh(bz) \right\} \exp\left(i\frac{1}{2}\Delta kz\right), \end{aligned} \tag{7}$$

where

$$b = \sqrt{g^2 - \left(\frac{\Delta k}{2}\right)^2}. \tag{8}$$

Here b is the parametric gain term (that takes into account the phase mismatch).

The above expression can be achieved by applying the second quantization formalism in the nonlinear classical equation. For a detailed explanation, see Appendix.

After solving the operator equations, the next step is to calculate the expectation values of $\langle \hat{a}_s^\dagger(z)\hat{a}_s(z) \rangle$ for finding the number of photons for each mode:

$$\begin{aligned} &\langle \hat{a}_s^\dagger(L)\hat{a}_s(L) \rangle \\ &= \left\langle \hat{a}_s^\dagger(0)\hat{a}_s(0) \cosh^2(bL) \right. \\ &\quad + \hat{a}_s^\dagger(0)\hat{a}_s(0) \cosh(bL)i\frac{\Delta k}{2b} \sinh(bL) \\ &\quad + \hat{a}_s^\dagger(0)\hat{a}_i^\dagger(0) \cosh(bL)i\frac{g}{b} \sinh(bL) \\ &\quad - \hat{a}_s^\dagger(0)\hat{a}_s(0)i\frac{\Delta k}{2b} \sinh(bL)i\frac{\Delta k}{2b} \cosh(bL) \\ &\quad - \hat{a}_s^\dagger(0)\hat{a}_s(0)i\frac{\Delta k}{2b} \sinh(bL) \cosh(bL) \\ &\quad - \hat{a}_s^\dagger(0)\hat{a}_i^\dagger(0)i\frac{\Delta k}{2b} \sinh(bL)i\frac{g}{b} \sinh(bL) \\ &\quad - \hat{a}_i(0)\hat{a}_s(0)i\frac{g}{b} \sinh(bL) \cosh(bL) \\ &\quad - \hat{a}_i(0)\hat{a}_s(0)i\frac{g}{b} \sinh(bL)i\frac{\Delta k}{2b} \sinh(bL) \\ &\quad \left. - \hat{a}_i(0)\hat{a}_i^\dagger(0)i\frac{g}{b} \sinh(bL)i\frac{g}{b} \sinh(bL) \right\}. \end{aligned} \tag{9}$$

Using some commutation relations from (4) and the normalization condition

$$\langle 0|\hat{a}_s\hat{a}_s^\dagger|0\rangle = \langle 0|\hat{a}_i\hat{a}_i^\dagger|0\rangle = 1, \quad (10)$$

one obtains the expectation values of the photon numbers for the signal (n_s) and idler (n_i) at the end of the crystal:

$$\begin{aligned} \bar{n}_s(L) &= \langle 0|\hat{a}_1^\dagger(L)\hat{a}_1(L)|0\rangle, \\ \bar{n}_i(L) &= \langle 0|\hat{a}_2^\dagger(L)\hat{a}_2(L)|0\rangle, \end{aligned} \quad (11)$$

$$\bar{n}_s(L) = \bar{n}_i(L) = \left(\frac{g}{b}\right)^2 \sinh^2(bL),$$

where $|0\rangle$ is the vacuum state of the system. Owing to the symmetric role of the signal and idler, the expectation values of their photon numbers are identical.

In our theoretical model we use the Heisenberg equations of motion along the spatial propagation coordinate (z) in order to determine the average number of photons at the crystal output. We note that this derivation is different than that of Louisell et al., which was carried out along the time coordinate t . Since we are interested to find the evolution of the signal and idler fields along the crystal, we preferred to use the space picture formalism.

2.2 Approximate OPG power estimation (identical gain model)

The new expression was derived based on crystal parameters such as length, width, gain bandwidth and crystal material. In this model we assumed that all modes that propagate in the gain bandwidth of the nonlinear crystal have the same gain and the same interaction length. All these assumptions simplified the model and brought the analytical expression:

$$P_{\text{signal}} = P_0 \left(\frac{g}{b}\right)^2 \sinh^2(bL) \exp(-\alpha_s L); \quad (12)$$

$$P_0 = dN \frac{hc^2}{n_s \lambda_s L},$$

where dN is the number of modes, which is given by the product of the density of modes in the frequency range of $\Delta\nu$ for a given polarization per steradian, with the interaction region subtending a solid angle $d\phi \approx d\phi_x d\phi_y$ and a mode volume of $V = \pi r^2 L$. The total number of modes that contribute to the effective noise in the signal (or idler) is estimated as [12]

$$dN = \pi r_p^2 L \frac{\nu^2}{c^3} \Delta\nu d\phi, \quad (13)$$

$$d\phi_x = d\phi_y = L_x/L_{\text{crystal}}, \quad (14)$$

where L_x is the width of the crystal (about 1-mm thick) and $d\phi_x$ and $d\phi_y$ are the full geometrical diffraction angles in each dimension.

In this model the phase-mismatch term that determined the value of the parametric gain term b was calculated by considering the first and second derivatives of the wave-vector with respect to the frequency [11]:

$$\begin{aligned} \Delta k &= \left(\frac{1}{u_s} - \frac{1}{u_i}\right) \delta\omega + \frac{1}{2}(g_s + g_i) \delta\omega^2, \\ \delta\omega &\approx \frac{2\pi}{L_{\text{crystal}} \left(\frac{1}{u_s} - \frac{1}{u_i}\right)}, \end{aligned} \quad (15)$$

where $\delta\omega$ is the gain bandwidth of the crystal, $u_n = (\partial k_n / \partial \omega_n)^{-1}$ is the group velocity of the signal or idler and $g_n = \partial^2 k_n / \partial \omega_n^2$ is the group velocity dispersion.

2.2.1 Discrete summation over all the modes

However, in order to obtain a realistic estimate of the generated power, one has to take into account the contributions of all the modes. We have found that in a typical OPG there are many modes (around 10^4). The number of modes is estimated by calculating the signal spectrum of an OPG configuration [8] and dividing the result by the density of modes of the bandwidth of the OPG.

The most accurate manner to consider the contributions of modes is to simply add one by one the contributions of all the modes that have significant parametric gain. As is commonly done in radiation theory, we assume that the electric field is zero on the boundaries of a volume defined by the crystal length and the pump cross section. Along the propagation direction z , this simply means that the ratio of the crystal length and half of the optical wavelength is an integer number (standing-wave condition, e.g. the z component of the signal wave-vector satisfies $k_{s,z} = m_{s,z} \pi / L$, where $m_{s,z}$ is an integer, as illustrated in Fig. 1). In the two transverse directions (X and Y) one has to consider the shape of the pump beam, which is usually circular (with a radius denoted by r_p), thereby defining a cylindrical volume. However, since usually the result depends only on the volume of the area, we can replace the cylindrical volume with a box, whose transverse size in both X - and Y -directions is $\sqrt{\pi r_p^2}$. In this case, the two transverse components of the wave-vector satisfy $k_{s,x} = j_{s,x} \pi / \sqrt{\pi r_p^2}$, $k_{s,y} = l_{s,y} \pi / \sqrt{\pi r_p^2}$, and $j_{s,x}, l_{s,y}$ are integers. Hence, for a given mode of the signal, the wave-vector is

$$\vec{k}_s = m_{sz} \frac{\pi}{L} \hat{z} + j_{sx} \frac{\pi}{\sqrt{\pi r_p^2}} \hat{x} + l_{sy} \frac{\pi}{\sqrt{\pi r_p^2}} \hat{y}. \quad (16)$$

And, the wave-vector for a given mode of the idler is given by

$$\vec{k}_i = m_{iz} \frac{\pi}{L} \hat{z} + j_{ix} \frac{\pi}{\sqrt{\pi r_p^2}} \hat{x} + l_{iy} \frac{\pi}{\sqrt{\pi r_p^2}} \hat{y}. \quad (17)$$

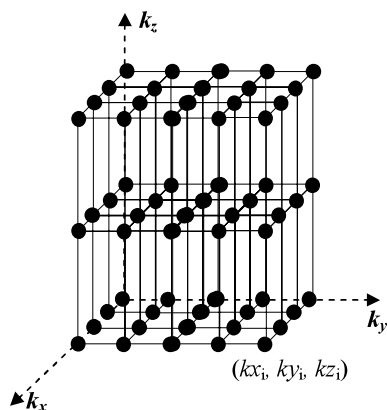


Fig. 1 Normal mode diagram. Each triple set of integers (m, l, j) represents a respective mode number

Hence, the vectorial phase mismatch can be easily calculated.

To find the output power, the summation is done over the all relevant modes. The spacing between each mode in a given direction is inversely proportional to the width of the crystal along that direction ((16) and (17)).

The OPG configuration is an unseeded amplifier which initiates from the quantum noise under the restriction of the phase-matching condition. In such a parametric process the generated wavelengths can propagate in collinear, as well as in non-collinear, directions with respect to the pump wave. Since the transverse beam size of the pump is finite, the overlap between the propagating waves and the pump due to non-collinear propagation reduces the crystal gain. The pump beam profile having a waist of r_p of 195 μm for the PPLN crystal and 150 μm for the PPSLT crystal is assumed to be unchanged along the interaction length because the Rayleigh range (~ 260 and ~ 420 mm, respectively) is much larger than the crystal length.

In this model we used a weighting function to calculate the gain reduction factor of the parametric process. We set the effective interaction length, $L_{\text{effective}}$, as a weighting function of the model. Since different modes have different propagation directions, the effective interaction length should be calculated separately for each mode.

The algorithm for calculating the effective length, $L_{\text{effective}}$, is based on geometrical considerations illustrated in Fig. 2, and is given by

$$L_{\text{effective}} = \begin{cases} L_{\text{crystal}} - \frac{L_{\text{crystal}}^2 \tan(\phi_{\text{signal}})}{4r_p}, & 0 \leq \phi_{\text{signal}} \leq \phi_{\text{crystal}}, \\ \frac{r_p}{\tan(\phi_{\text{signal}})}, & \phi_{\text{signal}} > \phi_{\text{crystal}}; \end{cases} \tag{18}$$

$$\phi_{\text{crystal}} = \frac{2r_p}{L_{\text{crystal}}}, \quad \phi_{\text{signal}} = \tan^{-1} \left(\frac{\sqrt{k_{sx}^2 + k_{sy}^2}}{k_{sz}} \right).$$

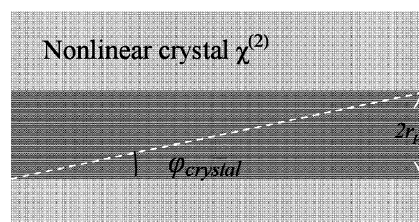


Fig. 2 The different parameters for calculating $L_{\text{effective}}$. The dark area represents the pump beam, whereas the dotted line is the direction of the generated signal wave

Here ϕ_{crystal} is an angle defined by the pump wave, whereas ϕ_{signal} is defined by the signal wave.

One can now calculate the total signal power by summing over all the relevant modes:

$$P_{\text{signal}} = \sum_{\lambda_s} \sum_{\pm m_{sz}, \pm j_{sy}, \pm l_{sz}} \sum_{\pm m_{iz}, \pm j_{iy}, \pm l_{iz}} P_{0\lambda_s} \left(\frac{g}{b} \right)^2 \times \sinh^2(bL_{\text{effective}}) \exp(-\alpha_s L_{\text{effective}}). \tag{19}$$

To estimate the initial conditions of the above expression, we calculated the power density of a single photon and then multiplied it by the beam area of the field to find the power of a single photon:

$$P_0 = \frac{hc^2}{n_s \lambda_s L}. \tag{20}$$

The last expression on the right-hand side of (19) was added in order to take into account the signal absorption in the crystal.

2.3 Continuous integration over beam parameters and pump frequency

This model was presented in [8], and its basic assumptions are the following: the theoretical analysis relies on Byer and Harris’s work [3], with the following improvements: (a) an accurate expression for the two-dimensional phase-mismatch term was used; (b) a weighting function was added to limit the phase-mismatch angle; (c) a non-diffracting Gaussian beam profile was assumed in the transverse direction; (d) a Gaussian pulse was assumed in the time domain. Using this improved model, we derived a single analytic equation that can be integrated to derive the OPG output power.

To find the output energy, the number of generated photons is integrated over all the relevant modes. The numbers of modes in the frequency range $-\Delta\omega$ to $+\Delta\omega$ and diffraction angles ϕ_x and ϕ_z are calculated, depending on the wave number k . The pump interacts with all the possible modes. The total output energy is obtained by summing over the frequencies and angles, and over the pump cross section and

temporal profile. The pump is assumed to be undepleted in power, and its beam profile, having a waist of w_0 , is assumed to be unchanged along the interaction length because the Rayleigh range is much larger than the crystal. In the time domain, a Gaussian pulse of length t_0 is assumed.

In this paper we compare the integration over the pump frequency and beam parameter approach (model C) [8] and the summation over discrete modes theory (model A).

3 Experimental details

The experimental setup consists of a Nd:YVO₄ Q-switched laser (at 1.064- μm wavelength), with 25-ns pulse length and 10-kHz repetition rate. The laser is linearly polarized, and its beam quality is $M^2 < 1.1$. The pump power was controlled with a $\lambda/2$ retardation wave plate and a polarizer. The pump beam was focused into the center of the nonlinear crystal to a beam waist radius of 195 μm for the PPLN crystal and 150 μm for the PPSLT crystal. In this experiment we used four different crystals: 25-, 35- and 42-mm-long PPLN crystals and 47-mm-long PPSLT crystals. The near-stoichiometric lithium tantalate crystals were produced from congruent lithium tantalate by a vapor-transport equilibration process [13]. In all three crystals the thickness was 1 mm. The poling periods were 28 and 29.4 μm for the LiNbO₃ and the stoichiometric LiTaO₃ crystals, respectively. The phase-matched signal and idler wavelengths were 1.45 and 1.48 μm for the signal and 4 and 3.8 μm for the idler.

The 35- and the 42-mm crystal facets were polished at 5° with respect to the domain walls at the entrance and exit facets, respectively, to prevent oscillation of the generated fields within the crystal. The facets of the 25- and 47-mm crystals were parallel; in this case we rotate the crystal with respect to the domain walls to prevent oscillation of the signal. The crystals were placed in an oven and heated (to avoid photorefractive damage) to 150°C for the three crystals. The PPSLT crystal was tested at room temperature. To measure the output power of the signal, we inserted calibrated spectral filters into the OPG output beam.

4 Results and discussion

4.1 OPG output power

Figures 3 and 4 presents the measured and calculated signal output power obtained with two different PPLN and PPMgLN crystal lengths of 25 and 35 mm, respectively. Figure 5 shows the measured and calculated signal output power obtained with PPSLT crystal lengths of 47 mm. The refractive indices for the PPLN and the periodically poled

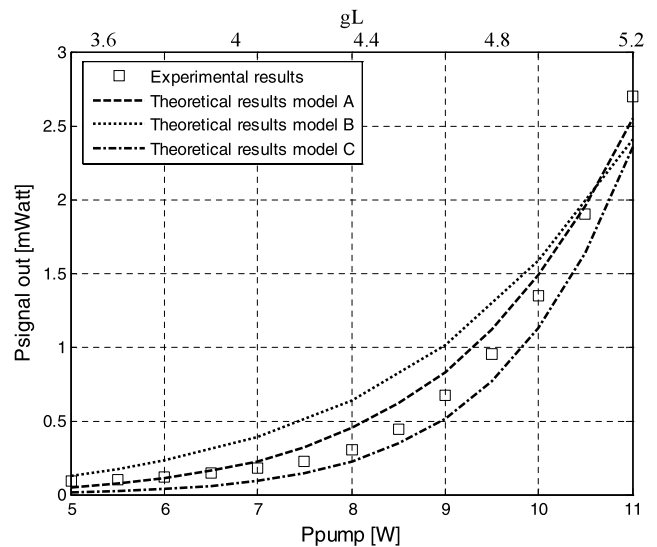


Fig. 3 Measured and calculated average OPG output powers for 25-mm-long PPLN crystal at different pump levels

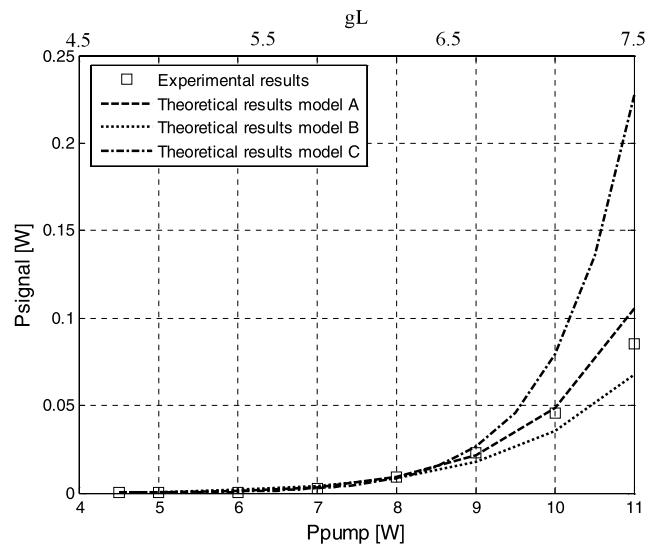


Fig. 4 Measured and calculated average OPG output powers for 35-mm-long PPLN crystal at different pump levels

stoichiometric lithium tantalite (PPSLT) crystals were calculated by the Sellmeier equation of Dmitriev et al. [14] and Bruner et al. [15], respectively. For the nonlinear coefficient, we assumed that $d_{\text{eff}} = 14.5$ pm/V for the PPLN crystals and $d_{\text{eff}} = 9$ pm/V for the PPSLT crystals. We do not know in advance the nonlinear coefficient of each crystal, since it depends on the poling quality. For an ideal crystal, with identical size positive and negative domains, the value of the nonlinear coefficient should be $d_{33}(2/\pi)$ (which is 17 pm/V for lithium niobate [16] and 9.5 pm/V for SLT [17]), but any deviation from that pattern reduces the effective nonlinear coefficient. Owing to the very sharp dependence of the OPG power on this value (it determines the argument of the sinh

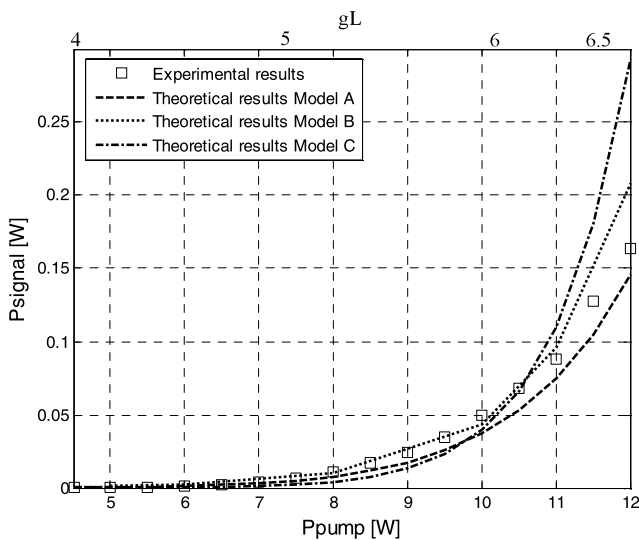


Fig. 5 Measured and calculated average OPG output powers for 47-mm-long PPSLT crystal at different pump levels

function), we consider it as a fitting parameter of the model. The d_{eff} that was obtained is quite close to the theoretical values for ideal crystals, indicating a high-quality poling.

As can be seen, models A and B describe well the experimental results for the entire pump intensity range we measured.

In model A the signal output power was calculated by summing all the modes that are found in the gain bandwidth of the nonlinear crystal. The modes were calculated by using the crystal and the pump beam dimensions. The gain bandwidth was considered by using the first and the second derivatives of the phase-mismatch term.

In model B the signal power was calculated by summing over all the wavelengths and modes in each crystal. The model takes into account the parametric gain term of non-collinear modes and calculates the effective interaction length over which the nonlinear interaction takes place.

In this work we compare the new results (models A and B) and our previous work (model C) [8]. To make a reasonable comparison between the models, the nonlinear coefficient was set to 14.5 pm/V for the PPLN crystal for all three models and 9 pm/V for the PPSLT crystal. At low pump power, model C showed a good agreement between the experimental results and the theoretical model, but for higher values of gain-length product a discrepancy from the theoretical model is observed (Figs. 4 and 5). We have found that the new models have a good agreement up to a gain-length product of $gL \leq 7.5$. Since the new models (A and B) fit well the results of Figs. 3–5, whereas our previous model works only for the short PPLN crystal (the case of Fig. 3), the new models offer a significant improvement in predicting the behavior of OPGs.

In our previous work [8], we have found that the model is valid for $gL \leq 10$. In that case the value of the nonlinear

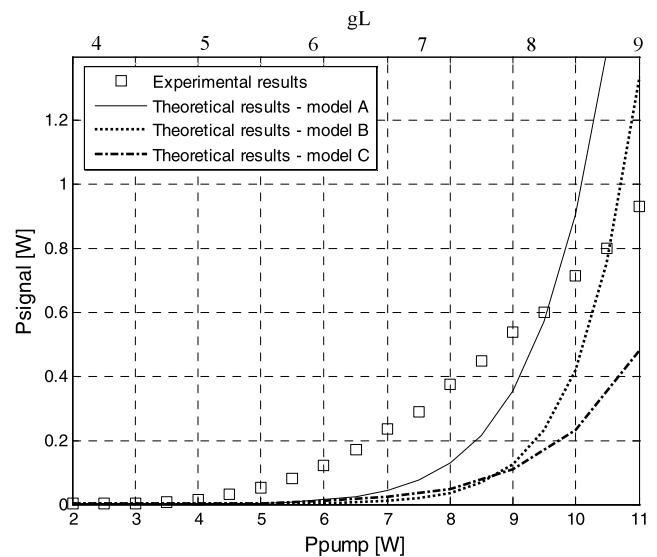


Fig. 6 Measured and calculated average OPG output powers for 42-mm-long PPLN crystal at different pump levels. Theory—solid line, experiment— $L = 42$ mm (squares)

coefficient (which was taken as a free parameter) was set to 17 pm/V. As was pointed out in the above paragraph, the validity range of the models has a strong dependence on the nonlinear coefficient value. Since in this work the nonlinear coefficient was set to a lower value (14.5 pm/V), the validity range of the new models seems to be lower even though it has a good agreement for all of the pump intensity range that was measured, including pump power levels in which the previous model [8] did not show agreement with the experiments.

Figure 6 shows the measured and calculated signal output power in a 42-mm-long PPLN crystal. At a very low pump power (up to $gL \approx 5.5$) there is reasonable agreement between the experimental results and the developed theory. When the pump power increases, a discrepancy from the theoretical model is revealed. A possible cause may be the variation of the nonlinear coefficient along the crystal. Owing to the ‘exploding’ nature of the sinh function, even small deviations could lead to significant variations at the output power. Such deviations are more likely to occur in longer crystals; hence, using a single fixed value of the nonlinear coefficient, as was done in our calculation, may not be sufficient. In addition, as we noted above, the losses of the signal and idler are not taken into account in our model, but the losses of the idler wave in this experiment are in fact quite significant.

5 Summary and conclusions

We derived new analytical models for analyzing OPG behavior for the parametric process for deriving the number of

photons per mode and on radiation theory for determining the mode density and wave-vectors of the different modes. The identical gain model shows a good agreement between the experimental data and the theoretical model. A comparison between the integration over continuous modes approach versus the discrete modes summation was made and we found the second model more accurate and matches the experimental results for an extended range.

The new models show better agreement with the experimental results with respect to previous theory that did not take into account the quantized nature of the electromagnetic modes and calculated the power by integrating over the beam parameters, rather than the mode number.

It was shown that the new models predict well the OPG power for 25- and 35-mm-long PPLN crystal and for 47-mm-long PPSLT crystal for the entire pump intensity range we measured.

We still could not find any agreement between the developed theories and the experimental results for long crystals (above 35 mm) with high nonlinearity (PPLN crystals). Possible causes may be the variation of the nonlinear coefficient along the crystal or the idler losses, which are not taken into account in our model. Owing to the ‘exploding’ nature of the sinh function, even small deviations could lead to significant variations of the output power.

Appendix

The expectation value for the mode number of a single electromagnetic mode is based on a slight modification of the quantum mechanical derivation for parametric processes that was developed by Louisell et al. [1]. The equations of motion were obtained directly from the classical parametric equations. For a non-depleted pump wave the two coupled-wave equations that determine the evolution of the signal and idler waves become linear equations. A quantum mechanical model is obtained by replacing the signal and idler field amplitudes with creation and annihilation operators (in the Heisenberg representation) for two lossless modes, coupled by a classical harmonically varying term. We start from the classical equations [9]

$$\begin{aligned} \frac{dA_s}{dz} &= i\kappa_s A_p A_i^* \exp(-i\Delta kz), \\ \frac{dA_i^*}{dz} &= -i\kappa_i A_p^* A_s \exp(i\Delta kz), \\ \kappa_{s,i} &= \frac{\omega_{s,i} d_{\text{eff}}}{n_{s,i} c}, \end{aligned} \tag{A.1}$$

where A_s and A_i and their complex conjugates are classical slowly varying amplitudes and the subscripts s and i denote the signal and idler waves. A_p is the amplitude of the

pump, which is assumed to be undepleted. $\Delta \vec{k} = \Delta k \cdot \hat{z} = \vec{k}_p - \vec{k}_s - \vec{k}_i - \vec{k}_{\text{QPM}}$ is a vector which is assumed to be in the propagation direction z , k_p , k_s and k_i are the pump, signal and idler wave-vectors and $\vec{k}_{\text{QPM}} = (2\pi/\Lambda)\hat{z}$ is the quasi-phase-matched reciprocal vector, Λ is the modulation period of the nonlinear coefficient, ω_i is the angular frequency, d_{eff} is the quadratic nonlinear coefficient, n_i is the refractive index, c is the velocity of light and $\kappa_{i,s}$ is the coupling coefficient.

By using the transformation from classical variables to quantum mechanical operators:

$$\begin{aligned} A_s &\rightarrow \hat{a}_s, & A_s^* &\rightarrow \hat{a}_s^\dagger, \\ A_i &\rightarrow \hat{a}_i, & A_i^* &\rightarrow \hat{a}_i^\dagger, \end{aligned} \tag{A.2}$$

the operator equation can be written as

$$\begin{aligned} \frac{d\hat{a}_s}{dz} &= i\kappa_s A_p \hat{a}_i^\dagger \exp(-i\Delta kz), \\ \frac{d\hat{a}_i^\dagger}{dz} &= -i\kappa_i A_p^* \hat{a}_s \exp(i\Delta kz). \end{aligned} \tag{A.3}$$

In (A.3), $\hat{a}_s^\dagger(z)$ and $\hat{a}_i^\dagger(z)$ are the creation operators, for the signal and idler modes, respectively. Note that (A.3) represent the variation along the propagation axis z , rather than the time parameter t used in Louisell et al. [1]. The operators should satisfy the following commutation relations as in (5).

The expectation values $\langle \hat{a}_s^\dagger(z) \hat{a}_s(z) \rangle$ and $\langle \hat{a}_i^\dagger(z) \hat{a}_i(z) \rangle$ represent the flux of the photon numbers for the signal and idler, respectively. It is important to notice that any two operators belonging to different modes commute and also annihilation operators (creation operators) commute with annihilation operators (creation operators).

In order to determine the OPG output power, we need to calculate only the number of photons in the signal and idler modes at a distance $z = L$ of the crystal, where the initial state at $z = 0$ is the vacuum state $|0\rangle$. It should be noted that while the classical amplitudes for our case vanish at $z = 0$, $\hat{a}_s(0)$ and $\hat{a}_i^\dagger(0)$ represent quantum input operators, and the calculation of any expectation value (corresponding to classical measurement) might depend on the order of operators. Any initial operator $\hat{a}_s(0)$ or $\hat{a}_i(0)$ operating directly to the right on the ket vacuum state $|0\rangle$ vanishes. Any initial operator $\hat{a}_s^\dagger(0)$ or $\hat{a}_i^\dagger(0)$ operating directly to the left on the bra state $\langle 0|$ vanishes. The solution of the two operator equations (A.3) is given by

$$\begin{aligned} \hat{a}_s(z) &= \left\{ \hat{a}_s(0) \left[\cosh(bz) + i \frac{\Delta k}{2b} \sinh(bz) \right] \right. \\ &\quad \left. + i \frac{g}{b} \hat{a}_i^\dagger(0) \sinh(bz) \right\} \exp\left(-i \frac{1}{2} \Delta kz\right), \\ \hat{a}_i^\dagger(z) &= \left\{ \hat{a}_i^\dagger(0) \left[\cosh(bz) - i \frac{\Delta k}{2b} \sinh(bz) \right] \right. \\ &\quad \left. - i \frac{g}{b} \hat{a}_s(0) \sinh(bz) \right\} \exp\left(i \frac{1}{2} \Delta kz\right), \end{aligned} \tag{A.4}$$

where the b and g parameters are defined in (8) and (5), respectively.

References

1. W.H. Louisell, A. Yariv, A.E. Siegman, *Phys. Rev.* **124**, 1646 (1961)
2. T.G. Giallorenzi, C.L. Tang, *Phys. Rev.* **166**, 225 (1967)
3. R.L. Byer, S.E. Harris, *Phys. Rev.* **168**, 1064 (1968)
4. W.G. Wagner, R.W. Hellwarth, *Phys. Rev.* **133**, A915 (1963)
5. D. Magde, H. Mahr, *Phys. Rev. Lett.* **18**, 905 (1967)
6. R.G. Smith, J.G. Skinner, J.E. Geusic, W.G. Nilsen, *Phys. Rev. Lett.* **12**, 97 (1968)
7. Y.R. Shen, *The Principles of Nonlinear Optics* (Wiley-Interscience, New York, 1984)
8. S. Acco, P. Blau, A. Arie, *Opt. Lett.* **33**, 1264 (2008)
9. Y.B. Aryeh, *Phys. Lett. A* **328**, 306 (2004)
10. B. Huttner, S. Serulnik, Y. Ben-Aryeh, *Phys. Rev. A* **42**, 5594 (1990)
11. R.L. Byer, in *Quantum Electronics: A Treatise*, ed. by H. Rabin and C.L. Tang (Academic Press, New York, 1975), pp. 587–702
12. W.H. Louisell, *Radiation and Noise in Quantum Electronics* (McGraw-Hill, New York, 1964)
13. M. Katz, R.K. Route, D.S. Hum, K.R. Parameswaran, G.D. Miller, M.M. Fejer, *Opt. Lett.* **29**, 1775 (2004)
14. V.G. Dmitriev, G.G. Gurzadyan, D.N. Nikogosyan, *Handbook of Nonlinear Optical Crystals*, 3rd edn. (Springer, Berlin, 1999)
15. A. Bruner, D. Eger, M.B. Oron, P. Blau, M. Katz, S. Ruschin, *Opt. Lett.* **28**, 194 (2003)
16. M.M. Fejer, G.A. Magel, D.H. Jundt, R.L. Byer, *IEEE J. Quantum Electron.* **28**, 2631 (1992)
17. N.E. Yu, S. Kurimura, Y. Nomura, M. Nakamura, K. Kitamura, Y. Takada, J. Sakuma, T. Sumiyoshi, *Appl. Phys. Lett.* **85**, 5134 (2004)